Prefrontal single-unit firing associated with deficient extinction in mice

Paul J Fitzgerald[a,*], **Nigel Whittle**[b], **Shaun M Flynn**[a], **Carolyn Graybeal**[a], **Courtney Pinard**[a], **Ozge Gunduz-Cinar**[a], **Alexxai Kravitz**[c], **Nicolas Singewald**[b], and **Andrew Holmes**[a]

[a]Laboratory of Behavioral and Genomic Neuroscience, National Institute on Alcohol Abuse and Alcoholism, NIH, Bethesda, MD, USA

[b]Department of Pharmacology & Toxicology, Institute of Pharmacy and CMBI, University of Innsbruck, Innsbruck, Austria

[c]National Institute of Diabetes and Digestive and Kidney Diseases, NIH, Bethesda, MD, USA

Abstract

The neural circuitry mediating fear extinction has been increasingly well studied and delineated. The rodent infralimbic subregion (IL) of the ventromedial prefrontal cortex (vmPFC) has been found to promote extinction, whereas the prelimbic cortex (PL) demonstrates an opposing, pro-fear, function. Studies employing in vivo electrophysiological recordings have observed that while increased IL single-unit firing and bursting predicts robust extinction retrieval, increased PL firing can correlate with sustained fear and poor extinction. These relationships between single-unit firing and extinction do not hold under all experimental conditions, however. In the current study, we further investigated the relationship between vmPFC and PL single-unit firing and extinction using inbred mouse models of intact (C57BL/6J, B6) and deficient (129S1/SvImJ, S1) extinction strains. Simultaneous single-unit recordings were made in the PL and vmPFC (encompassing IL) as B6 and S1 mice performed extinction training and retrieval. Impaired extinction retrieval in S1 mice was associated with elevated PL single-unit firing, as compared to firing in extinguishing B6 mice, consistent with the hypothesized pro-fear contribution of PL. Analysis of local field potentials also revealed significantly higher gamma power in the PL of Sthan B6 mice during extinction training and retrieval. In the vmPFC, impaired extinction in S1 mice was also associated with exaggerated single-unit firing, relative to B6 mice. This is in apparent contradiction to evidence that IL activity promotes extinction, but could reflect a (failed) compensatory effort by the vmPFC to mitigate fear-promoting activity in other regions, such as the PL or amygdala. In support of this hypothesis, augmenting IL activity via direct infusion of the $GABA_A$ receptor antagonist picrotoxin rescued impaired extinction retrieval in S1 mice. Chronic fluoxetine treatment produced modest reductions in fear during extinction retrieval and increased the number of Zif268-labeled cells in layer II of IL, but failed to increase vmPFC single-unit

*Corresponding author. Tel.: +1 443 564 1306. pfitz@mbi.mb.jhu.edu.

firing. Collectively, these findings further support the important contribution these cortical regions play in determining the balance between robust extinction on the one hand, and sustained fear on the other. Elucidating the precise nature of these roles could help inform understanding of the pathophysiology of fear-related anxiety disorders.

Keywords

fear extinction; retrieval; C57BL/6J; 129S1/SvImJ; picrotoxin; fluoxetine; infralimbic cortex; prelimbic cortex; Zif268; medial prefrontal cortex; local field potential; gamma oscillations; cross correlation

Introduction

Fear extinction has emerged as a tractable experimental assay for studying the neuropathophysiology and therapeutic alleviation of disorders characterized by impaired extinction, such as phobias and posttraumatic stress disorder (PTSD) (Holmes & Quirk, 2010; Andero & Ressler, 2012; Milad & Quirk, 2012). Our understanding of extinction has been greatly facilitated in recent years by the delineation of neural circuitry mediating extinction in rodents. Major roles have been ascribed to the rodent medial prefrontal cortex (mPFC), hippocampus and amygdala (Herry et al., 2010; Pape & Pare, 2010; Orsini & Maren, 2012), with analogous regions of the human brain also being recruited during extinction (Milad & Quirk, 2012).

An informative approach to dissecting the neural correlates of extinction in rodents has been in vivo single-unit recordings to measure extinction-related neuronal activity in specific brain regions, with a particular emphasis on the mPFC and amygdala. A pioneering study by Milad and Quirk revealed a significant increase in neuronal activity in the rat infralimbic (IL) subregion of mPFC in rats retrieving an extinction memory (Milad & Quirk, 2002). This and subsequent studies have found that the magnitude of increases in IL neuronal firing and/or bursting correlate with the degree to which extinction memories are retrieved (Milad & Quirk, 2002; Burgos-Robles et al., 2007; Wilber et al., 2011; Holmes et al., 2012). Conversely, neurons in the rat prelimbic (PL) mPFC subregion can exhibit sustained firing during fear expression and this activity predicts poor extinction retrieval (Burgos-Robles et al., 2009; Sotres-Bayon et al., 2012).

Further supporting a functional role for mPFC neuronal firing in extinction, experimental manipulations that impair extinction retrieval produce parallel shifts in tone-elicited IL and PL neuronal firing. For example, mice (C57BL/6J strain) exposed to chronic alcohol exhibit poor extinction retrieval and a corresponding reduction of neuronal firing and bursting in a vmPFC region encompassing IL (Holmes et al., 2012). Likewise, in rats with deficient extinction retrieval following exposure to chronic restraint stress, IL neurons showed loss of increases in firing, whereas PL neurons failed to exhibit the normal decrease in firing observed in non-stressed controls (Wilber et al., 2011). These data are consistent with a depression of IL neuronal firing, and a parallel increase in PL firing, under conditions of impaired extinction retrieval. This is in agreement with some but not all data derived from other techniques (e.g., pharmacological, lesion, electrical stimulation) that support ‘pro-

extinction' versus 'pro-fear' functions of the IL and PL, respectively (Milad & Quirk, 2012; Courtin et al., 2013). Of particular relevance are studies using immediate-early gene (IEG) mapping of the regional recruitment of neuronal activity. Expression of the IEGs c-Fos and Zif268 is relatively high in IL and relatively low in PL in rats and mice exhibiting good extinction learning and/or retrieval (e.g., Hefner et al., 2008; Kim et al., 2010; Whittle et al., 2010; Knapska et al., 2012). Beyond these convergent findings, however, there are currently some inconsistencies in the literature. For example, some single-unit recording studies have reported that impaired extinction retrieval, due to performing extinction training soon after conditioning, is associated with increased IL neuronal firing (Chang et al., 2010), rather than the converse.

Here we sought to extend the literature by taking advantage of populations of mice that exhibit marked differences in extinction and assessed whether these differences were paralleled by divergent extinction-related mPFC single-unit activity. Previous studies have shown that the 129S1/SvImJ (S1) inbred mouse strain has a profound deficit in extinction, while the C57BL/6J (B6) inbred strain typically exhibits robust extinction (Hefner et al., 2008; Camp et al., 2009). These strain differences in extinction extend to measures of safety learning, HPA-axis abnormalities and neuronal dendritic morphology, and are coupled to IL hypoactivity and PL hyperactivity, as demonstrated by IEG mapping (Hefner et al., 2008; Camp et al., 2009; Whittle et al., 2010; Camp et al., 2012; Whittle et al., 2013). Here, we performed simultaneous single-unit recordings of extinction-related activity in B6 and S1 mice within the PL and the vmPFC region encompassing IL. The role of the IL in deficient extinction was further tested by pharmacologically activating (via picrotoxin infusion) the region in S1 mice prior to extinction. We then examined whether the abnormal single-unit activity we observed in the vmPFC of S1 mice could be normalized by a treatment, chronic fluoxetine, that rescues extinction retrieval in this strain (Camp et al., 2012). We also quantified IEG (Zif268) expression in the IL of the same mice we recorded from, to provide a direct comparison between patterns of in vivo single-unit activity and region-wide IEG expression.

Materials and Methods

Subjects

Subjects were male S1 and B6 mice obtained at ~8–9 weeks of age from The Jackson Laboratory (Bar Harbor, ME). Mice were single-housed post-surgery in a temperature (72 ± 5°F) and humidity (45 ± 15%) controlled vivarium under a 12 hour light/dark cycle (lights on 0600 h). The number of mice used in each experiment is given in the figure legends. All procedures were approved by the NIAAA Animal Care and Use Committee or the Austrian Animal Experimentation Ethics Board (Bundesministerium für Wissenschaft und Verkehr, Kommission für Tierversuchsangelegenheiten), and followed the NIH guidelines outlined in 'Using Animals in Intramural Research.'

Fear conditioning and extinction

Testing consisted of 3 phases: conditioning, extinction training and extinction retrieval. Freezing (no visible movement except that required for breathing) was manually scored

every 5 seconds as an index of fear (Blanchard and Blanchard, 1969), and converted to a percentage [(number of freezing observations/total number of observations) × 100].

Conditioning was conducted in Context A: a 27 × 27 × 11 cm chamber with transparent walls and a metal rod floor, cleaned with a 79.5% water/19.5% ethanol/1% vanilla-extract solution. After a 180-second baseline period, mice received 3 × pairing(s) of a 30-second, 75–80 dB, white noise conditioned stimulus (CS) and 2 sec, 0.6 mA scrambled footshock [unconditioned stimulus (US)], in which the US was presented during the last 2 seconds of the CS and the inter-trial-interval (ITI) was variable. There was a 120-second no-stimulus period after the final pairing before mice were returned to the home cage. Stimulus presentation was controlled by the Med Associates VideoFreeze system (Med Associates, Burlington, VT, USA).

Extinction training was conducted the day after conditioning (except for the fluoxetine experiments - see below), in Context B: a 20 cm-diameter Plexiglas cylinder with black/white-checkered walls, solid-Plexiglas opaque floor, cleaned with a 99% water/1% acetic acid solution, located in a different room from Context A. After a 180-second baseline period, there were 50 × CS presentations, with a 5-sec inter-CS interval. The following day, extinction retrieval was tested in Context B. After a 180-second baseline period, mice received 5 × 30-second non-reinforced CS presentations (5 second inter-CS interval).

Electrode implantation

One to 2 weeks prior to testing, mice were anesthetized with isoflurane and placed in a stereotaxic alignment system (Kopf Instruments, Tujunga, CA, USA) for electrode implantation and in vivo single-unit recordings, as previously described (Brigman et al., 2013; DePoy & Holmes, 2013). The scalp was retracted and a 2 × 2 mm portion of skull removed to allow implantation of a microelectrode array, which was stabilized with dental cement (Coralite Dental Products, Skokie, IL, USA).

To co-target vmPFC and PL, a fixed 8 × 2-row array (200 μm spacing between rows) of tungsten microelectrodes (Innovative Neurophysiology, Durham, NC, USA) was inserted lengthwise anteroposterior (35 μm diameter, 150 μm spacing between electrodes within a row) in the right hemisphere. The coordinates for the center of the array were anteroposterior +1.7–2.0 mm and mediolateral +0.35–0.5 μm from Bregma skull surface. To target PL, one row was fabricated the electrodes +0.25 mm in length and targeted to −2.3 dorsoventral and +0.25 mm mediolateral from Bregma. The vmPFC-targeting row was fabricated with a longer, 5.0 mm, electrodes and targeted to −2.9 dorsoventral and +0.45 mm mediolateral from Bregma. Because the anteroposterior extent of the mouse IL is lesser than PL, it is likely that the anterior-most microelectrodes of the arrays were positioned in medial orbital cortex – hence we refer to these as vmPFC.

In a separate experiment, to target vmPFC alone, the surgical procedure and array parameters were the same as above (electrode length 5.0 mm), except that arrays were either implanted in the right hemisphere (row spacing and coordinates as above) or, in order to target vmPFC bilaterally, the 2 rows spacing was increased to 1000 μm and each was

implanted into a separate hemisphere (+5.0 mm mediolateral from Bregma). However, as no hemispheric differences in unit activity were evident, data were combined.

To verify electrode placements at the completion of testing, mice were terminally anesthetized with ketamine/xylazine, and lesions made at the tips of the recording electrodes by passing currents that were typically 50–100 μA for 20 sec (S48 Stimulator and Model CCU1, Grass Technologies, West Warwick, RI, USA). Mice were transcardially perfused with 4% paraformaldehyde solution in phosphate buffer and brains removed. Fifty μm coronal sections were cut with a vibratome (Classic 1000 model, Vibratome, Bannockburn, IL, USA) and stained with cresyl violet. Lesion sites were estimated with the aid of an Olympus (Center Valley, PA, USA) BX41 microscope.

In vivo recordings

Single-unit activity was recorded during early extinction (first 5-trials of extinction training), late extinction (last 5-trials of extinction training), and extinction retrieval (Figure 1A). No assumptions were made about recording from the same units across phases. Electrical waveforms larger than a user-adjusted voltage threshold were digitized at 40 kHz (16 channel Multichannel Acquisition Processor, Plexon, Dallas, TX, USA) and stored in a computer. Waveforms were sorted off-line using 2-dimensional plots of principal components, and we marked waveform clusters in these plots with contours (Offline Sorter, Plexon). Timestamps of action potentials and the beginning and end of auditory tones were imported to NeuroExplorer (Nex Technologies, Littleton, MA) for analysis and graphical display. Note that no attempts were made to categorize cells based upon firing rate and waveform duration.

The average (1-sec) pre-CS firing of recorded neurons across experiments was quite high (5.05 Hz for vmPFC, 6.36 Hz for PL), likely reflecting the inclusion of a proportion of fast-spiking interneurons. Recorded cells typically had excitatory (as opposed to inhibitory) CS-evoked response profiles. Data were analyzed in 50 msec time bins for the 1-sec baseline period prior to the CS, and the 2-sec post-CS epoch. A baseline-normalized Z score was calculated for each 50 msec bin, and group peri-event time histograms were created by averaging the scores of all recorded units. Additionally, the average Z score for the first 100-msec post-CS timebin and the average of the whole 2-sec post-CS period were separately analyzed. Strain, region and drug treatment effects were analyzed using 2-factor analysis of variance (with repeated measures for time) and unpaired Student's t-test.

Cross-correlations of single-unit activity were calculated from the recordings that were performed simultaneously in vmPFC and PL. Cross-correlations during the 2-sec post-CS period were calculated using Neuroexplorer for activity: 1) between PL units, 2) between vmPFC units and 3) between vmPFC and PL units. Cross-correlations were also calculated during a 2-sec pre-CS ITI period. Activity was analyzed in 2-msec bins across a 200-msec window around a reference spike. The peak correlation (maximum spikes/bin) within the window was determined for each spike-spike comparison and used to calculate the average of peak values in all units. Strain effects were analyzed using unpaired Student's t-test.

Local field potential (LFP) waveforms were sampled at 1 kHz, pre-amplified at 1000× and low-pass filtered at 250 Hz. The Power Spectral Density (PSD) of each LFP was calculated with the NeuroExplorer PSD function. PSD values were expressed as the percent of the total power spectrum. LFPs were binned in to 0.1 Hz bins and smoothed using a post-processing filter width of 5 bins. The maximal % power density within the theta (5–8 Hz) and gamma (30–50 Hz) ranges were determined for each strain and test-phase and analyzed using 2-factor analysis of variance. Representative spectrograms of the power density of LFP activity were plotted using the perievent spectrogram function in NeuroExplorer (waveforms high-pass filtered at 4 Hz,, frequency binned into 0.05 Hz bins for theta activity and into 0.20 Hz bins for gamma activity).

Effects of pharmacological activation of IL

One to 2 weeks prior to testing, mice underwent stereotaxic surgery (as above) to implant 26-gauge bilateral guide cannulas (Plastics One, Roanoke, VA, USA) targeted at the IL (+1.40 mm anteroposterior, ±0.40 mm mediolateral, −2.00 mm ventral to Bregma) and held in place with dental cement. Thirty minutes prior to extinction training, mice were infused with 0.1 μL of 10 ng per hemisphere of the $GABA_A$ receptor antagonist picrotoxin (Sigma-Aldrich, St. Louis, MO, USA) or an equivalent volume of saline/0.5% DMSO vehicle. Bilateral 33-gauge injectors (Plastics One) were inserted into the guide cannulas and drugs slowly infused over a 90-second period using a syringe pump (Harvard Apparatus PHD 22/2000, Holliston, MA, USA), with injectors left in place for a further 2 minutes to allow diffusion.

To verify cannula placements at the completion of testing, mice were terminally anesthetized with ketamine/xylazine, transcardially perfused with 4% paraformaldehyde solution in phosphate buffer and brains removed. Fifty μm coronal sections were cut with a vibratome (Leica VT1000S, Buffalo Grove, IL, USA) and stained with cresyl violet. Cannula placements were estimated with the aid of an Olympus (Center Valley, PA, USA) BX41 microscope.

Fluoxetine effects on extinction-related vmPFC IEG expression and single-unit activity

Recent studies have shown that chronic fluoxetine treatment facilitates extinction retrieval in B6 (Karpova et al., 2012) and S1 (Camp et al., 2012) mice. We took advantage of this effect to test whether improvements in extinction memory in S1 mice could be associated with normalization of the abnormal patterns of vmPFC single-unit firing (see Results) shown by these mice. Mice were provided with 120 mg/L fluoxetine (FLX) hydrochloride (LKT Laboratories Inc, St. Paul, MN) in (their only source of) drinking water, as previously described (Brigman et al., 2010). The dose and concentration was chosen based on previous data from our laboratory (Holmes & Rodgers, 2003; Karlsson et al., 2008; Norcross et al., 2008) to attain an average self-administered daily dose of ~10 mg/kg. Non-treated controls received water alone and solutions were refreshed weekly. Fluoxetine and water consumption was measured from bottle weights (corrected for evaporation and spillage) and converted to a mg/kg body weight daily dose. Mice were conditioned then immediately started treatment. Extinction training was conducted 21 days later, and mice remained on treatment through to the completion of retrieval testing the following day.

Extinction-related single-unit firing was recorded from multi-channel electrode arrays implanted in the vmPFC (right hemisphere) of S1 mice, as described above. We have previously found that rescue of impaired extinction retrieval in S1 mice (by dietary zinc depletion) is paralleled by a normalization of IL hypoactivity, as evidenced by quantification of the immediate-early genes (IEGs) c-Fos and Zif268 (Hefner et al., 2008; Whittle et al., 2010). We first sought to confirm that extinction facilitation produced by fluoxetine treatment had a similar effect on IEG expression in the IL. Two hours after the completion of retrieval testing, mice were terminally anesthetized with ketamine/xylazine, and brains removed and snap frozen. Brains were sectioned in the coronal plane at 50 μm thickness on a vibratome (VT1000S, Leica Microsystems, Buffalo Grove, IL, USA) and collected in immunobuffer. The free-floating sections were processed for Zif268-like immunoreactivity as described previously (Hefner et al., 2008; Whittle et al., 2009), via incubation with a polyclonal primary antibody (1:5000; sc-189; Santa Cruz Biotechnology, Dallas, TX, USA) and a biotinylated goat anti-rabbit secondary antibody (1:200; Vector Laboratories). The anatomical localization of Zif268-positive cells was aided by reference to prior publications (Van De Werd et al., 2010) and a stereotaxic atlas (Paxinos & Franklin, 2001).

Results

Extinction-related vmPFC and PL single-unit activity

Three mice were excluded from the analysis due to misplaced electrodes (1 placed too ventrally, 2 placed too laterally) resulting in final group sizes of 6–7 per strain (for final placements, see Figure 1B). Behavioral analysis showed that S1 mice froze more than B6 during late extinction ($t(11) = 5.13$, $P<.01$) and retrieval ($t(11) = 6.09$, $P<.01$), but not early extinction (Figure 1C).

In PL, recordings were made from 55–65 units per test phase and strain. There was significantly higher post-CS firing in S1 mice than B6 mice period extinction retrieval ($t(114) = 2.43$, $P<.05$), but not early or late extinction (Figure 2A–E). In addition, firing was elevated during retrieval in S1 mice ($F2,136 = 3.21$, $P<.05$, retrieval versus late extinction via Fisher's LSD post hoc tests), but did not change across phases in B6 mice. Analyses of firing patterns in 50-msec bins revealed a significant interaction between strain and time for early extinction ($F59,7257 = 1.75$, $P<.01$), late extinction ($F59,7257 = 1.45$, $P<.05$), and retrieval ($F59,6726 = 1.38$, $P<.05$). There most clearly discernible pattern was higher firing in S1 mice that was sustained across the post-CS period during extinction retrieval (Figure 2B–F). Activity during the first 100 msec post-CS did not differ between strains for any phase of testing (Figure 2B–F, inset).

In vmPFC, recordings were made from 43–52 units per test phase and strain. There was significantly higher post-CS firing in S1 mice than B6 mice during early, not late, extinction ($t(97) = 2.01$, $P<.05$), with a non-significant trend in the same direction during extinction retrieval (Figure 3A–E). In addition, firing was highest during retrieval in B6 ($F2,136 = 3.21$, $P<.05$, retrieval versus late extinction via Fisher's LSD post hoc tests) and S1 mice ($F2,151 = 3.94$, $P<.05$, retrieval versus late extinction via Fisher's LSD post hoc tests). Time course analysis indicated a significant interaction between strain and time for early extinction ($F59,5723 = 1.48$, $P<.05$), and a significant effect of time for late extinction

(F1,59 = 2.52, $P<.01$) and retrieval (F1,59 = 5.65, $P<.01$). S1 mice had higher firing than B6 mice particularly during the latter part of the post-CS epoch (Figure 3B–F), and activity did not differ between strains on any phase during the first 100 msec post-CS (Figure 3B–F, inset).

Cross-correlational analysis of unit activity within the PL indicated a significant main effect of strain (F2,3963 = 7.20, $P<.01$). Although there was no strain × test-phase interaction, post hoc analyses were conducted based on the phase-specific strain differences in freezing. Correlations among PL units were significantly higher in S1 than B6 mice during extinction retrieval, but not other phases (Figure 4A). For units within the vmPFC, there was a significant effect of strain (F1,2484 = 53.31, $P<.01$) and test phase (F2,2484 = 13.34, $P<.01$). Correlations were significantly higher in S1 than B6 mice during all test phases, and significantly higher in both S1 and B6 mice during retrieval than early extinction (Figure 4B). Comparison of units across PL and vmPFC revealed a significant strain × test phase interaction (F2,5922 = 8.26, $P<.01$). Correlations between the regions were significantly higher in S1 than B6 mice during all test phases, and significantly higher in both S1 and B6 mice during retrieval relative to early extinction (Figure 4C). During the pre-tone period, PL unit correlations did not differ with strain or test phase. Pre-tone, vmPFC units correlated more in S1 than B6 mice during all phases (strain effect: F1,2485 = 28.56, $P<.01$, followed by post hoc tests) and more in both strains during extinction retrieval than early extinction (effect of test phase: F2,2485 = 5.39, $P<.01$, followed by post hoc tests). Finally, pre-tone vmPFC-PL correlations were higher in S1 than B6 mice during all phases (strain effect: F1,5921 = 19.56, $P<.01$, followed by post hoc tests) and more in both strains during extinction retrieval than early extinction (effect of test phase: F2,5921 = 40.94, $P<.01$, followed by post hoc tests).

To confirm that the strain differences in cross-correlated activity were not simply a reflection of differences in underlying unit firing, we compared the firing rate of the strains at each phase of testing. Firing rate in the PL did not differ between strains at any testing phase (Figure 4D), while firing was significantly higher in S1 mice than B6 during extinction retrieval (t(93)=2.02, $P<.05$), but not early or late extinction training (Figure 4E). Therefore, the strain differences in cross-correlations, which are evident across test phases, for both PL and vmPFC, cannot be solely explained by differences in the underlying firing rate. Example cross-correlograms of two vmPFC S1 units and two vmPFC B6 units are shown in Figure 4F.

LFP analysis revealed a significant effect of strain, not phase, in gamma (F1,33 = 13.27, $P<.01$) but not theta, oscillations in the PL – due to higher gamma frequency in S1 mice at each phase of testing, relative to B6 mice (Figure 5A–D). By contrast, during context exposure in unconditioned mice, gamma power in the PL was no different between strains (Figure S2). There was no significant effect of strain or phase for gamma or theta oscillations in the vmPFC (Figure 5E–H).

Replication of abnormal extinction-related vmPFC single-unit activity

We sought to confirm the (unexpected – see Discussion) finding that vmPFC single-unit activity was higher in the extinction-impaired S1 strain, than the extinction-intact B6 strain

in an independent experiment in which arrays were implanted in vmPFC alone and extinction retrieval was conducted days after training to bolster fear (spontaneous recovery). Two mice were excluded from this experiment due to misplaced electrodes (1 placed too dorsally and 1 placed too ventrally) (for final placements, see Figure S1A), resulting in final group sizes of 6–9 per strain. Behavioral analysis showed that B6 mice froze more to the first CS during conditioning than S1 mice (B6 = 15.6 ± 4.4, S1= 2.9 ± 2.9, t(14) = 2.24, $P<.05$), and S1 mice froze more than B6 during late extinction (B6 = 41.5 ± 7.2, S1= 88.1 ± 5.4, t(14) = 4.94, $P<.01$) and retrieval (B6 = 61.1 ± 3.6, S1= 80.0 ± 5.1, t(14) = 3.10, $P<.05$), but not early extinction (B6 = 78.1 ± 7.7, S1= 79.0 ± 8.0). Recordings were made from 37–72 units per test phase and strain. There was a significant interaction between strain and time for early extinction (F59,7847 = 2.69, $P<.01$), late extinction (F59,7670 = 1.48, $P<.05$), and retrieval (F59,4838 = 2.10, $P<.01$) (Figure S3). Activity also differed between strains during the first 100 msec post-CS on early extinction (t(133) = 3.23, $P<.01$), late extinction (t(130) = 2.57, $P<.05$) and extinction retrieval (t(82) = 2.22, $P<.05$) (Figure S3, inset). Finally, examination of the 2-sec post-CS period as a whole revealed significantly higher firing in S1 mice than B6 mice during early extinction (t(133) = 4.38, $P<.01$), late extinction (t(130) = 2.88, $P<.01$) and extinction retrieval (t(82) = 2.65, $P<.01$) (Figure S3). In addition, firing was highest during retrieval in B6 (F2,151 = 3.94, $P<.05$, retrieval versus early and late extinction via Fisher's LSD post hoc tests) and S1 mice (F2,190 = 9.52, $P<.01$, retrieval versus early and late extinction via Fisher's LSD post hoc tests).

Effects of pharmacological activation of IL

S1 mice infused with picrotoxin (for infusion sites, see Figure 6A) showed a significant reduction in freezing during early (t(15) = 2.25, $P<.05$), but not late, extinction, as compared to vehicle controls. Picrotoxin-infused mice froze significantly less than vehicle controls during extinction retrieval (t(15) = 3.12, $P<.01$) (Figure 6B).

Extinction-related vmPFC single-unit activity and IEG expression following fluoxetine treatment

One mouse was excluded from the analysis due to misplaced electrodes (too ventral, in the dorsal peduncular region) and another for having an outlying (+2 SD) fear score, resulting in final group sizes of 5–8 per treatment (for final placements, see Figure S1C). Mice given the fluoxetine-containing solution self-administered an average dose of 12.0 ± 0.4 mg/kg/day fluoxetine – achieving a dose similar to prior studies (Camp et al., 2012; Ihne et al., 2012).

Recordings were made from 82–136 units per test phase and treatment. There was significantly lower post-CS firing in fluoxetine-treated mice than water-treated controls during early extinction (t(218) = 2.46, $P<.05$), but not late extinction or extinction retrieval (Figure 7A–C). In addition, firing was highest during retrieval in water (F2,388 = 9.35, $P<.01$, retrieval versus late extinction via Fisher's LSD post hoc tests) and fluoxetine-treated mice (F2,262 = 5.04, $P<.01$, retrieval versus late extinction via Fisher's LSD post hoc tests). Time course analysis found a significant interaction between treatment and time for early extinction (F59,12862 = 2.34, $P<.01$) and a significant effect of time during late extinction (F59,13393 = 9.57, $P<.01$) and retrieval (F59,12095 = 18.57, $P<.01$). Further scrutiny of these data revealed higher firing in S1 mice than B6 mice during the latter part of the post-

CS period in early extinction (Figure 7B–F). Activity during the first 100 msec post-CS did not differ between treatment groups on early extinction, late extinction and extinction retrieval (Figure 7B–F, inset).

As previously reported (Camp et al., 2012), behavioral analyses showed that freezing did not differ between fluoxetine-treated mice and water controls during conditioning (trial 1: water = 2.5 ± 2.5, FLX = 8.0 ±4.9, trial 3: water = 62.5 ±5.9, FLX = 8.0 ± 4.9) or extinction (early: water = 78.8 ± 3.5, FLX = 70.7 ± 7.3, late: water = 69.3 ± 4.6, FLX = 69.3 ± 12.9), but was significantly lesser during extinction retrieval ($t(11) = 2.93$, $P<.05$) (Figure 8A). IEG analysis revealed a significantly higher number of Zif268-positive neurons in layer II ($t(11) = 4.22$, $P<.01$), but not layers III/V or VI, of the IL region of vmPFC of fluoxetine treated mice, as compared to water controls, after extinction retrieval (Figure 8B–D). Correlational analysis of the number of Zif268-positive cells in layer II of the IL correlated weakly with the amount of post-CS vmPFC unit firing during extinction retrieval ($r = 0.11$) (Figure 8E). In the PL, there were no significant differences between fluoxetine treated mice and water controls in Zif268-labeled neurons after extinction retrieval. The number of Zif268-positive cells in layer II of the PL correlated positively, but not significantly, ($r = 0.37$) with retrieval-related vmPFC single-unit firing (Figure 8F–G).

Discussion

The main objective of the current study was to identify patterns of extinction-related single-unit firing in the vmPFC and PL of two strains of inbred mice with divergent extinction. Results showed marked differences in the extinction-related single-unit activity and LFPs between the S1 and B6 strains and provide new insights into the contribution of these brain regions to differences in extinction.

Increased PL firing during impaired extinction retrieval in S1 mice

As previously reported (Hefner et al., 2008; Camp et al., 2009; Whittle et al., 2010; Camp et al., 2012; Gunduz-Cinar et al., 2013; Whittle et al., 2013), the S1 mouse strain exhibited impaired extinction, as compared to mice of the B6 strain. Here, using in vivo recordings we demonstrate that this S1 impairment in extinction retrieval is associated with exaggerated (relative to B6) single-unit firing in the PL region of the mPFC. This fits well with the recent finding that the failure to show extinction retrieval in S1 mice (and other models such as the ‘immediate extinction deficit’ (Stafford et al., 2013), is associated with increased IEG expression in the PL (Whittle et al., 2010). It also agrees well with prior studies in which rats with relatively poor extinction exhibited elevated PL firing during retrieval (Burgos-Robles et al., 2009; Wilber et al., 2011). Collectively, these data support a ‘pro-fear/extinction-opposing’ role for the PL (Vidal-Gonzalez et al., 2006; Courtin et al., 2013; Holmes & Singewald, 2013). The mechanisms involved are not fully understood. However, an elegant recent study by Sotres-Bayon and colleagues has shown that inactivation of the BLA greatly attenuated fear-related single-unit responses in the rat PL, thereby identifying BLA as a major source of excitatory drive to PL during high fear states (Sotres-Bayon et al., 2012). Interestingly, elevated PL unit firing in extinction-impaired S1 mice and stressed rats is associated with BLA abnormalities such as dendritic hypertrophy (Roozendaal et al.,

2009; Camp et al., 2012). In this regard, it would be valuable to test whether local manipulations of BLA (Gunduz-Cinar et al., 2013) that rescue extinction retrieval in S1 mice would also produce normalization in PL firing.

It should be noted that a pro-fear function of the PL is not evident under all experimental conditions. For example, rodents rendered extinction-impaired by chronic alcohol exposure or undergoing extinction training soon after fear conditioning (a phenomenon termed the 'immediate extinction effect,' that also occurs in mice (Macpherson et al., 2013) showed relatively low, rather than high, PL firing (Chang et al., 2010; Holmes et al., 2012). This suggests that PL hyperactivity is sufficient, but not necessary, for extinction to be impaired. Excessive PL drive therefore likely contributes to deficient extinction in some models, such as the S1 strain, while other abnormalities such as IL and/or BLA hypoactivity, may account for poor extinction in other cases. Providing additional support for this account, LFP analysis revealed markedly increased gamma power in the PL of S1 mice, across all phases of testing. Because gamma oscillations can reflect synchronized neuronal activity, synaptic plasticity and learning (Buzsaki & Wang, 2012), increased gamma power could be a further indication of a hyper-functional PL in S1 mice. Another possibility is that the increased PL gamma activity reflects heightened input from other regions within the fear/extinction circuit, such as the basal amygdala (BA) (Burgos-Robles et al., 2009). In this context, prior studies have found that reward-learning in cats is associated with greater coherence of gamma oscillations between the BA and striatum (Popescu et al., 2009). Finally, although theta power coherence between the lateral amygdala and IL has also been linked to fear extinction learning in mice (Lesting et al., 2011a; Lesting et al., 2011b; Narayanan et al., 2011), this was not specifically tested here and no strain differences in theta power within the PL or vmPFC per se were found.

'Paradoxical' vmPFC firing during high fear states in S1 mice

Recordings of single-units in B6 mice revealed that vmPFC firing was highest during extinction retrieval, as previously described in this strain (Holmes et al., 2012), and in rats (Sierra-Mercado et al., 2011; Wilber et al., 2011). S1 mice also had high firing during retrieval as compared to extinction training, and showed higher firing rates than in B6 mice. In contrast to B6 mice, however, vmPFC firing in S1 mice was high during test phases when units in B6 mice were relatively quiescent, notably during early extinction.

The profile of elevated vmPFC activity across test phases in extinction-impaired S1 mice appears to contradict previous studies pointing to the contribution of the IL to the acquisition, consolidation and retrieval of extinction, but not to fear expression (Milad & Quirk, 2012; Courtin et al., 2013). Prior studies conducted in either rats or B6 mice have reported a close correlation between increased IL neuronal firing (and/or bursting) and robust extinction retrieval (Milad & Quirk, 2002; Burgos-Robles et al., 2007; Holmes et al., 2012; Sotres-Bayon et al., 2012). These data have been interpreted as reflecting the encoding of extinction memories by IL neurons, and are supported by other lines of evidence. For example, temporary inactivation of the IL, via local infusion of the GABA receptor agonist muscimol, impairs extinction acquisition and retrieval (Sierra-Mercado et al., 2011), and IL-infusion of compounds that disrupt memory consolidation also produce

deficient extinction retrieval (e.g., Herry et al., 2006; Burgos-Robles et al., 2007; Holmes et al., 2012; Sepulveda-Orengo et al., 2013). Various environmental insults, including stress and alcohol exposure, also produce deficits in extinction in association with IL dendritic hypotrophy and attenuated IL single-unit firing (Izquierdo et al., 2006; Wilber et al., 2011; Holmes et al., 2012). Thus, on the basis of these findings, high IL unit firing in S1 mice seems paradoxical given the deficient extinction in the strain.

However, despite the overall convergence of evidence, not all studies have found a clear relationship between IL activity and extinction. An early study observed rat IL and PL neurons had highly heterogeneous cue-related responses (increased, decreased, no change) but, overall, showed reduced firing over the course of extinction training (Baeg et al., 2001). More recently, Chang et al. examined IL unit firing in rats rendered extinction-impaired by immediate extinction, and observed significantly augmented IL unit firing during extinction retrieval in the extinction-impaired rats, relative to a group tested with a normal conditioning-extinction delay (Chang et al., 2010). A possible explanation reconciling these observations is that there may be circumstances in which vmPFC single-units increase firing to attenuate hyperactivity in fear-promoting areas but effectively fail to dampen fear. It is unlikely that the increased vmPFC firing is an epiphenomenon unrelated to extinction in these mice because infusion of picrotoxin, a $GABA_A$ receptor antagonist that is predicted to increase neuronal activity, into IL was sufficient to transiently reduced fear during early extinction training and produced a marked decrease in fear during extinction retrieval. This concurs with earlier reports of extinction-facilitating effects of IL-picrotoxin in rats (Thompson et al., 2010; Chang & Maren, 2011) and indicates that by augmenting activity in the vmPFC, the region's contribution to extinction formation can be sufficiently strengthened to overcome extinction deficits in various models.

Although the identity of the putative fear-promoting regions that may drive compensatory vmPFC activity in S1 mice remains to be determined, there are a number of good candidates. One is the central medial nucleus of the amygdala (CeM), the main amygdala fear output nucleus. We have previously found that impaired extinction in S1 mice is associated with abnormally high IEG activity and dendritic hypertrophy in the CeM (MacPherson et al., unpublished observations; Hefner et al., 2008; Whittle et al., 2010). Another obvious candidate given the findings discussed above is the PL. To assess the contribution of PL hyperactivity to impaired extinction in S1 mice, it would be valuable to test whether PL ablation or inactivation would normalize vmPFC function and allow for the successful gating of extinction in S1 mice. The current data provide some, albeit less direct, insight into the functional interrelationship between the PL and vmPFC by showing that cross-correlated unit activity between the two regions was higher in S1 than B6 mice throughout testing, but particularly during extinction retrieval. Correlated activity was also greater in S1 mice between units within the vmPFC, and between PL units specifically during extinction retrieval. These patterns would be generally consistent with sustained excessive PL drive to vmPFC and the subsequent maintenance of fear during extinction.

vmPFC single-unit firing does not predict immediate-early gene expression

Chronic fluoxetine treatment did not affect fear during conditioning or extinction, but significantly reduced fear during extinction retrieval. This retrieval-specific effect of fluoxetine replicates previous findings in both the S1 and B6 mouse strains, as well as in rats (Deschaux et al., 2011; Camp et al., 2012; Karpova et al., 2012; Deschaux et al., 2013). The magnitude of the effect was noticeably lesser here, perhaps due to an effect of the in vivo recording procedure in this more stress-sensitive strain.

Nonetheless, modest facilitation of extinction retrieval by fluoxetine treatment produced a significant increase in expression of the IEG Zif268 in IL, though a caveat here is that Zif268 expression was only examined after retrieval and it remains possible that fluoxetine treatment would have produced a generalized increase in IL Zif268 expression across behavioral states. However, increased IL Zif268 expression after retrieval replicates our prior finding that IL hypoactivation is reversed by other treatments (e.g., dietary zinc restriction) that robustly rescue extinction in the S1 strain (Hefner et al., 2008; Whittle et al., 2010). A novel finding was the lack of any correlation between the increased IL Zif268 expression and the firing of single-units in the vmPFC.

An important qualification to this apparent lack of correlation is that IEG expression changes were specific to layer II of IL, whereas recordings were not restricted to any specific layer and spanned IL and the more anterior MO. Nonetheless, dissociation between IL single-unit firing and IEG expression is not without precedent. For example, rats with extinction impairments induced by ‘immediate’ (post-conditioning) extinction training show low IL IEG expression (Kim et al., 2010) but high IL single-unit firing (Chang et al., 2010) (albeit tested in different groups of rats). The expression of IEGs, particularly those involved in plasticity and memory formation such as Zif268 (Bozon et al., 2003), may reflect the functional recruitment of an ensemble of neurons that is a substrate of an extinction memory, akin to the neuronal substrates of fear memory reported in the BLA and hippocampus (Han et al., 2009; Garner et al., 2012; Liu et al., 2012). The current data, together with those of (Kim et al., 2010) and (Chang et al., 2010) suggest that recording from an essentially arbitrary sampling of single units, during a limited epoch, may not always accurately capture these regional network dynamics (Balaguer-Ballester et al., 2011). This is not surprising considering IEG data reflect the summation of sustained and coordinated activity of extinction-selective neurons over the course of retrieval as well the post-retrieval (re)consolidation period.

Supplementary Material

Refer to Web version on PubMed Central for supplementary material.

Acknowledgments

We are grateful to Dr. Cara Wellman for valuable comments. Research supported by the National Institute on Alcohol Abuse and Alcoholism Intramural Research Program and the Austrian Science Fund (SFB F4410-B19).

References

1. Andero R, Ressler KJ. Fear extinction and BDNF: translating animal models of PTSD to the clinic. Genes Brain Behav. 2012; 11:503–512. [PubMed: 22530815]
2. Baeg EH, Kim YB, Jang J, Kim HT, Mook-Jung I, Jung MW. Fast spiking and regular spiking neural correlates of fear conditioning in the medial prefrontal cortex of the rat. Cereb Cortex. 2001; 11:441–451. [PubMed: 11313296]
3. Balaguer-Ballester E, Lapish CC, Seamans JK, Durstewitz D. Attracting dynamics of frontal cortex ensembles during memory-guided decision-making. PLoS Comput Biol. 2011; 7:e1002057. [PubMed: 21625577]
4. Bozon B, Davis S, Laroche S. A requirement for the immediate early gene zif268 in reconsolidation of recognition memory after retrieval. Neuron. 2003; 40:695–701. [PubMed: 14622575]
5. Brigman JL, Daut RA, Wright T, Gunduz-Cinar O, Graybeal C, Davis MI, Jiang Z, Saksida LM, Jinde S, Pease M, Bussey TJ, Lovinger DM, Nakazawa K, Holmes A. GluN2B in corticostriatal circuits governs choice learning and choice shifting. Nat Neurosci. 2013; 16:1101–1110. [PubMed: 23831965]
6. Brigman JL, Mathur P, Harvey-White J, Izquierdo A, Saksida LM, Bussey TJ, Fox S, Deneris E, Murphy DL, Holmes A. Pharmacological or genetic inactivation of the serotonin transporter improves reversal learning in mice. Cereb Cortex. 2010; 20:1955–1963. [PubMed: 20032063]
7. Burgos-Robles A, Vidal-Gonzalez I, Quirk GJ. Sustained conditioned responses in prelimbic prefrontal neurons are correlated with fear expression and extinction failure. J Neurosci. 2009; 29:8474–8482. [PubMed: 19571138]
8. Burgos-Robles A, Vidal-Gonzalez I, Santini E, Quirk GJ. Consolidation of fear extinction requires NMDA receptor-dependent bursting in the ventromedial prefrontal cortex. Neuron. 2007; 53:871–880. [PubMed: 17359921]
9. Buzsaki G, Wang XJ. Mechanisms of gamma oscillations. Annu Rev Neurosci. 2012; 35:203–225. [PubMed: 22443509]
10. Camp M, Norcross M, Whittle N, Feyder M, D'Hanis W, Yilmazer-Hanke D, Singewald N, Holmes A. Impaired Pavlovian fear extinction is a common phenotype across genetic lineages of the 129 inbred mouse strain. Genes Brain Behav. 2009; 8:744–752. [PubMed: 19674120]
11. Camp MC, Macpherson KP, Lederle L, Graybeal C, Gaburro S, Debrouse LM, Ihne JL, Bravo JA, O'Connor RM, Ciocchi S, Wellman CL, Luthi A, Cryan JF, Singewald N, Holmes A. Genetic strain differences in learned fear inhibition associated with variation in neuroendocrine, autonomic, and amygdala dendritic phenotypes. Neuropsychopharmacology. 2012; 37:1534–1547. [PubMed: 22334122]
12. Chang CH, Berke JD, Maren S. Single-unit activity in the medial prefrontal cortex during immediate and delayed extinction of fear in rats. PLoS ONE. 2010; 5:e11971. [PubMed: 20700483]
13. Chang CH, Maren S. Medial prefrontal cortex activation facilitates re-extinction of fear in rats. Learn Mem. 2011; 18:221–225. [PubMed: 21430044]
14. Courtin J, Bienvenu TC, Einarsson EO, Herry C. Medial prefrontal cortex neuronal circuits in fear behavior. Neuroscience. 2013; 240:219–242. [PubMed: 23500092]
15. DePoy L, Holmes A. Chronic alcohol produces adaptations to prime dorsal striatal behavior. Proc Natl Acad Sci U S A. 2013
16. Deschaux O, Spennato G, Moreau JL, Garcia R. Chronic treatment with fluoxetine prevents the return of extinguished auditory-cued conditioned fear. Psychopharmacology (Berl). 2011; 215:231–237. [PubMed: 21181120]
17. Deschaux O, Zheng X, Lavigne J, Nachon O, Cleren C, Moreau JL, Garcia R. Post-extinction fluoxetine treatment prevents stress-induced reemergence of extinguished fear. Psychopharmacology (Berl). 2013; 225:209–216. [PubMed: 22825580]
18. Garner AR, Rowland DC, Hwang SY, Baumgaertel K, Roth BL, Kentros C, Mayford M. Generation of a synthetic memory trace. Science. 2012; 335:1513–1516. [PubMed: 22442487]
19. Gunduz-Cinar O, Macpherson KP, Cinar R, Gamble-George J, Sugden K, Williams B, Godlewski G, Ramikie TS, Gorka AX, Alapafuja SO, Nikas SP, Makriyannis A, Poulton R, Patel S, Hariri

AR, Caspi A, Moffitt TE, Kunos G, Holmes A. Convergent translational evidence of a role for anandamide in amygdala-mediated fear extinction, threat processing and stress-reactivity. Mol Psychiatry. 2013

20. Han JH, Kushner SA, Yiu AP, Hsiang HL, Buch T, Waisman A, Bontempi B, Neve RL, Frankland PW, Josselyn SA. Selective erasure of a fear memory. Science. 2009; 323:1492–1496. [PubMed: 19286560]
21. Hefner K, Whittle N, Juhasz J, Norcross M, Karlsson RM, Saksida LM, Bussey TJ, Singewald N, Holmes A. Impaired fear extinction learning and cortico-amygdala circuit abnormalities in a common genetic mouse strain. J Neurosci. 2008; 28:8074–8085. [PubMed: 18685032]
22. Herry C, Ferraguti F, Singewald N, Letzkus JJ, Ehrlich I, Luthi A. Neuronal circuits of fear extinction. Eur J Neurosci. 2010; 31:599–612. [PubMed: 20384807]
23. Herry C, Trifilieff P, Micheau J, Luthi A, Mons N. Extinction of auditory fear conditioning requires MAPK/ERK activation in the basolateral amygdala. Eur J Neurosci. 2006; 24:261–269. [PubMed: 16882022]
24. Holmes A, Fitzgerald PJ, Macpherson KP, Debrouse L, Colacicco G, Flynn SM, Masneuf S, Pleil KE, Li C, Marcinkiewcz CA, Kash TL, Gunduz-Cinar O, Camp M. Chronic alcohol remodels prefrontal neurons and disrupts NMDAR-mediated fear extinction encoding. Nat Neurosci. 2012; 15:1359–1361. [PubMed: 22941108]
25. Holmes A, Quirk GJ. Pharmacological facilitation of fear extinction and the search for adjunct treatments for anxiety disorders--the case of yohimbine. Trends Pharmacol Sci. 2010; 31:2–7. [PubMed: 20036429]
26. Holmes A, Rodgers RJ. Prior exposure to the elevated plus-maze sensitizes mice to the acute behavioral effects of fluoxetine and phenelzine. Eur J Pharmacol. 2003; 459:221–230. [PubMed: 12524150]
27. Holmes A, Singewald N. Individual differences in recovery from traumatic fear. Trends Neurosci. 2013; 36:23–31. [PubMed: 23260015]
28. Ihne JL, Fitzgerald PJ, Hefner KR, Holmes A. Pharmacological modulation of stress-induced behavioral changes in the light/dark exploration test in male C57BL/6J mice. Neuropharmacology. 2012; 62:464–473. [PubMed: 21906605]
29. Izquierdo A, Wellman CL, Holmes A. Brief uncontrollable stress causes dendritic retraction in infralimbic cortex and resistance to fear extinction in mice. J Neurosci. 2006; 26:5733–5738. [PubMed: 16723530]
30. Karlsson RM, Choe JS, Cameron HA, Thorsell A, Crawley JN, Holmes A, Heilig M. The neuropeptide Y Y1 receptor subtype is necessary for the anxiolytic-like effects of neuropeptide Y, but not the antidepressant-like effects of fluoxetine, in mice. Psychopharmacology (Berl). 2008; 195:547–557. [PubMed: 17891380]
31. Karpova NN, Pickenhagen A, Lindholm J, Tiraboschi E, Kulesskaya N, Agustsdottir A, Antila H, Popova D, Akamine Y, Bahi A, Sullivan R, Hen R, Drew LJ, Castren E. Fear erasure in mice requires synergy between antidepressant drugs and extinction training. Science. 2012; 334:1731–1734. [PubMed: 22194582]
32. Kim SC, Jo YS, Kim IH, Kim H, Choi JS. Lack of medial prefrontal cortex activation underlies the immediate extinction deficit. J Neurosci. 2010; 30:832–837. [PubMed: 20089891]
33. Knapska E, Macias M, Mikosz M, Nowak A, Owczarek D, Wawrzyniak M, Pieprzyk M, Cymerman IA, Werka T, Sheng M, Maren S, Jaworski J, Kaczmarek L. Functional anatomy of neural circuits regulating fear and extinction. Proc Natl Acad Sci U S A. 2012; 109:17093–17098. [PubMed: 23027931]
34. Lesting J, Geiger M, Narayanan RT, Pape HC, Seidenbecher T. Impaired extinction of fear and maintained amygdala-hippocampal theta synchrony in a mouse model of temporal lobe epilepsy. Epilepsia. 2011a; 52:337–346. [PubMed: 21054349]
35. Lesting J, Narayanan RT, Kluge C, Sangha S, Seidenbecher T, Pape HC. Patterns of coupled theta activity in amygdala-hippocampal-prefrontal cortical circuits during fear extinction. PLoS One. 2011b; 6:e21714. [PubMed: 21738775]

36. Liu X, Ramirez S, Pang PT, Puryear CB, Govindarajan A, Deisseroth K, Tonegawa S. Optogenetic stimulation of a hippocampal engram activates fear memory recall. Nature. 2012; 484:381–385. [PubMed: 22441246]
37. Macpherson KP, Whittle N, Camp M, Gunduz Cinar O, Singewald N, Holmes A. Temporal factors in the extinction of fear in inbred mouse strains differing in extinction efficacy. Biology of Mood and Anxiety Disorders. 2013
38. Milad MR, Quirk GJ. Neurons in medial prefrontal cortex signal memory for fear extinction. Nature. 2002; 420:70–74. [PubMed: 12422216]
39. Milad MR, Quirk GJ. Fear extinction as a model for translational neuroscience: ten years of progress. Annu Rev Psychol. 2012; 63:129–151. [PubMed: 22129456]
40. Narayanan V, Heiming RS, Jansen F, Lesting J, Sachser N, Pape HC, Seidenbecher T. Social defeat: impact on fear extinction and amygdala-prefrontal cortical theta synchrony in 5-HTT deficient mice. PLoS One. 2011; 6:e22600. [PubMed: 21818344]
41. Norcross M, Mathur P, Enoch AJ, Karlsson RM, Brigman JL, Cameron HA, Harvey-White J, Holmes A. Effects of adolescent fluoxetine treatment on fear-, anxiety- or stress-related behaviors in C57BL/6J or BALB/cJ mice. Psychopharmacology (Berl). 2008; 200:413–424. [PubMed: 18594797]
42. Orsini CA, Maren S. Neural and cellular mechanisms of fear and extinction memory formation. Neurosci Biobehav Rev. 2012; 36:1773–1802. [PubMed: 22230704]
43. Pape HC, Pare D. Plastic synaptic networks of the amygdala for the acquisition, expression, and extinction of conditioned fear. Physiol Rev. 2010; 90:419–463. [PubMed: 20393190]
44. Paxinos, KBJ.; Franklin, G. The mouse brain in stereotaxic coordinates. London: Academic Press; 2001.
45. Popescu AT, Popa D, Pare D. Coherent gamma oscillations couple the amygdala and striatum during learning. Nat Neurosci. 2009; 12:801–807. [PubMed: 19430471]
46. Roozendaal B, McEwen BS, Chattarji S. Stress, memory and the amygdala. Nat Rev Neurosci. 2009; 10:423–433. [PubMed: 19469026]
47. Sepulveda-Orengo MT, Lopez AV, Soler-Cedeno O, Porter JT. Fear Extinction Induces mGluR5-Mediated Synaptic and Intrinsic Plasticity in Infralimbic Neurons. J Neurosci. 2013; 33:7184–7193. [PubMed: 23616528]
48. Sierra-Mercado D, Padilla-Coreano N, Quirk GJ. Dissociable roles of prelimbic and infralimbic cortices, ventral hippocampus, and basolateral amygdala in the expression and extinction of conditioned fear. Neuropsychopharmacology. 2011; 36:529–538. [PubMed: 20962768]
49. Sotres-Bayon F, Sierra-Mercado D, Pardilla-Delgado E, Quirk GJ. Gating of fear in prelimbic cortex by hippocampal and amygdala inputs. Neuron. 2012; 76:804–812. [PubMed: 23177964]
50. Stafford JM, Maughan DK, Ilioi EC, Lattal KM. Exposure to a fearful context during periods of memory plasticity impairs extinction via hyperactivation of frontal-amygdalar circuits. Learn Mem. 2013; 20:156–163. [PubMed: 23422280]
51. Thompson BM, Baratta MV, Biedenkapp JC, Rudy JW, Watkins LR, Maier SF. Activation of the infralimbic cortex in a fear context enhances extinction learning. Learn Mem. 2010; 17:591–599. [PubMed: 21041382]
52. Van De Werd HJ, Rajkowska G, Evers P, Uylings HB. Cytoarchitectonic and chemoarchitectonic characterization of the prefrontal cortical areas in the mouse. Brain Struct Funct. 2010; 214:339–353. [PubMed: 20221886]
53. Vidal-Gonzalez I, Vidal-Gonzalez B, Rauch SL, Quirk GJ. Microstimulation reveals opposing influences of prelimbic and infralimbic cortex on the expression of conditioned fear. Learn Mem. 2006; 13:728–733. [PubMed: 17142302]
54. Whittle N, Hauschild M, Lubec G, Holmes A, Singewald N. Rescue of impaired fear extinction and normalization of cortico-amygdala circuit dysfunction in a genetic mouse model by dietary zinc restriction. J Neurosci. 2010; 30:13586–13596. [PubMed: 20943900]
55. Whittle N, Lubec G, Singewald N. Zinc deficiency induces enhanced depression-like behaviour and altered limbic activation reversed by antidepressant treatment in mice. Amino Acids. 2009; 36:147–158. [PubMed: 18975044]

56. Whittle N, Schmuckermair C, Gunduz Cinar O, Hauschild M, Ferraguti F, Holmes A, Singewald N. Deep brain stimulation, histone deacetylase inhibitors and glutamatergic drugs rescue resistance to fear extinction in a genetic mouse model. Neuropharmacology. 2013; 64:414–423. [PubMed: 22722028]

57. Wilber AA, Walker AG, Southwood CJ, Farrell MR, Lin GL, Rebec GV, Wellman CL. Chronic stress alters neural activity in medial prefrontal cortex during retrieval of extinction. Neuroscience. 2011; 174:115–131. [PubMed: 21044660]

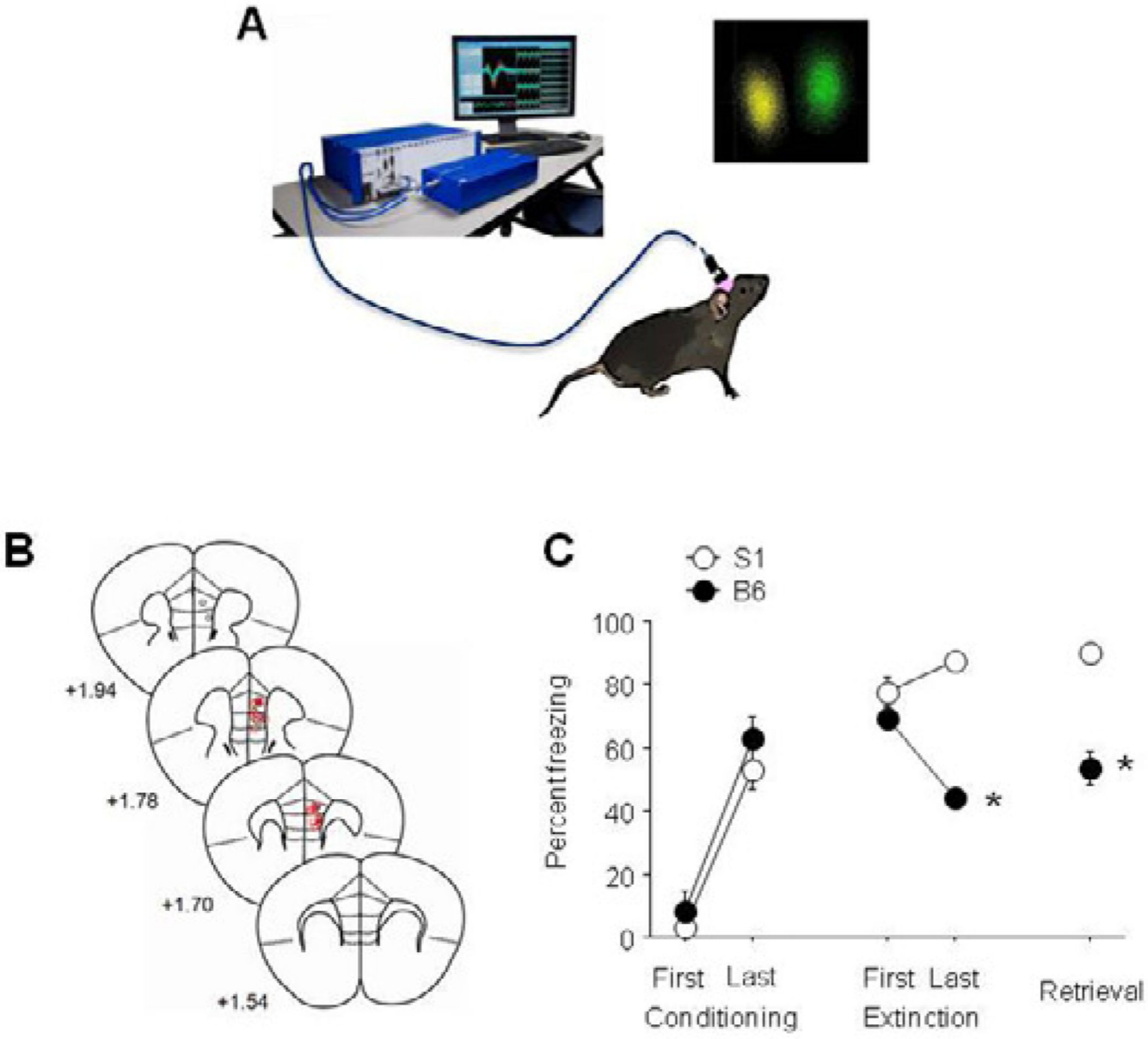

Figure 1. Extinction-related mPFC single-unit recordings in the extinguishing B6 strain and the non-extinguishing S1 strain

(**A**) Cartoon illustrating set-up for single-unit recording during fear extinction, and example of isolated units. (**B**) Estimated microelectrode array placements. (**C**) Freezing behavior showing extinction in B6 mice and impaired extinction in S1 mice (n=6–7 mice per strain). Data are Means ± SEM. * $P<.05$ versus B6/same task-phase.

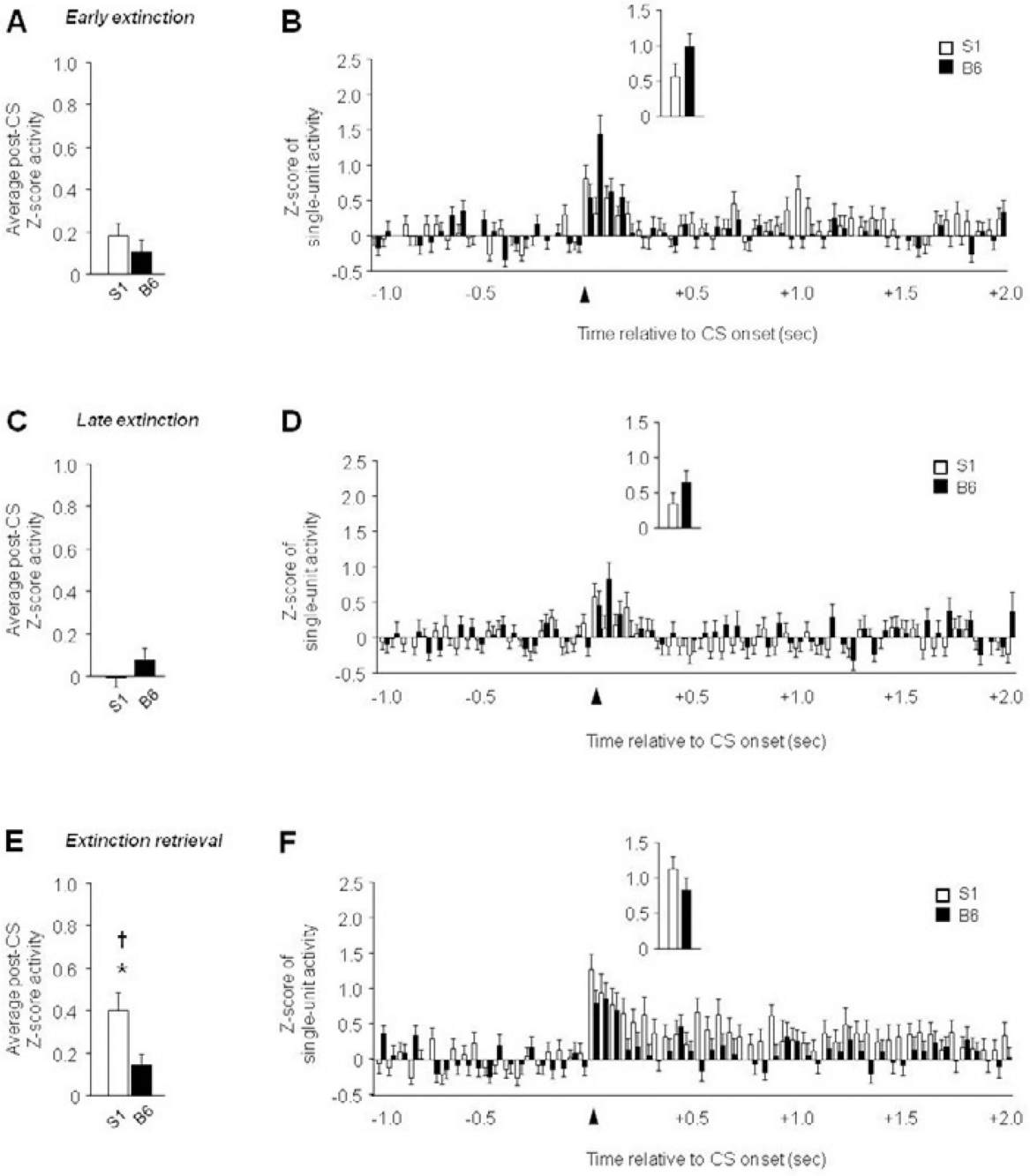

Figure 2. Increased PL single-unit activity during extinction retrieval in extinction-impaired S1 mice

(**A**) Average post-CS-related single-unit firing during early extinction. (**B**) Peri-event histogram of CS-related single-unit firing during early extinction (first 100 msec, inset). (**C**) Average post-CS-related single-unit firing during late extinction. (**D**) Peri-event histogram of CS-related single-unit firing during late extinction (first 100 msec, inset). (**E**) Higher average post-CS-related single-unit firing during extinction retrieval in S1 mice, relative to B6 mice, and higher firing during retrieval than late extinction in S1 mice. (**F**) Peri-event

histogram of CS-related single-unit firing during extinction retrieval (first 100 msec, inset). n=6–7 mice per strain, n=55–65 units per test phase and strain. Data are Means ± SEM. * $P<.05$ versus B6/same task-phase, † $P<.05$ retrieval versus late extinction.

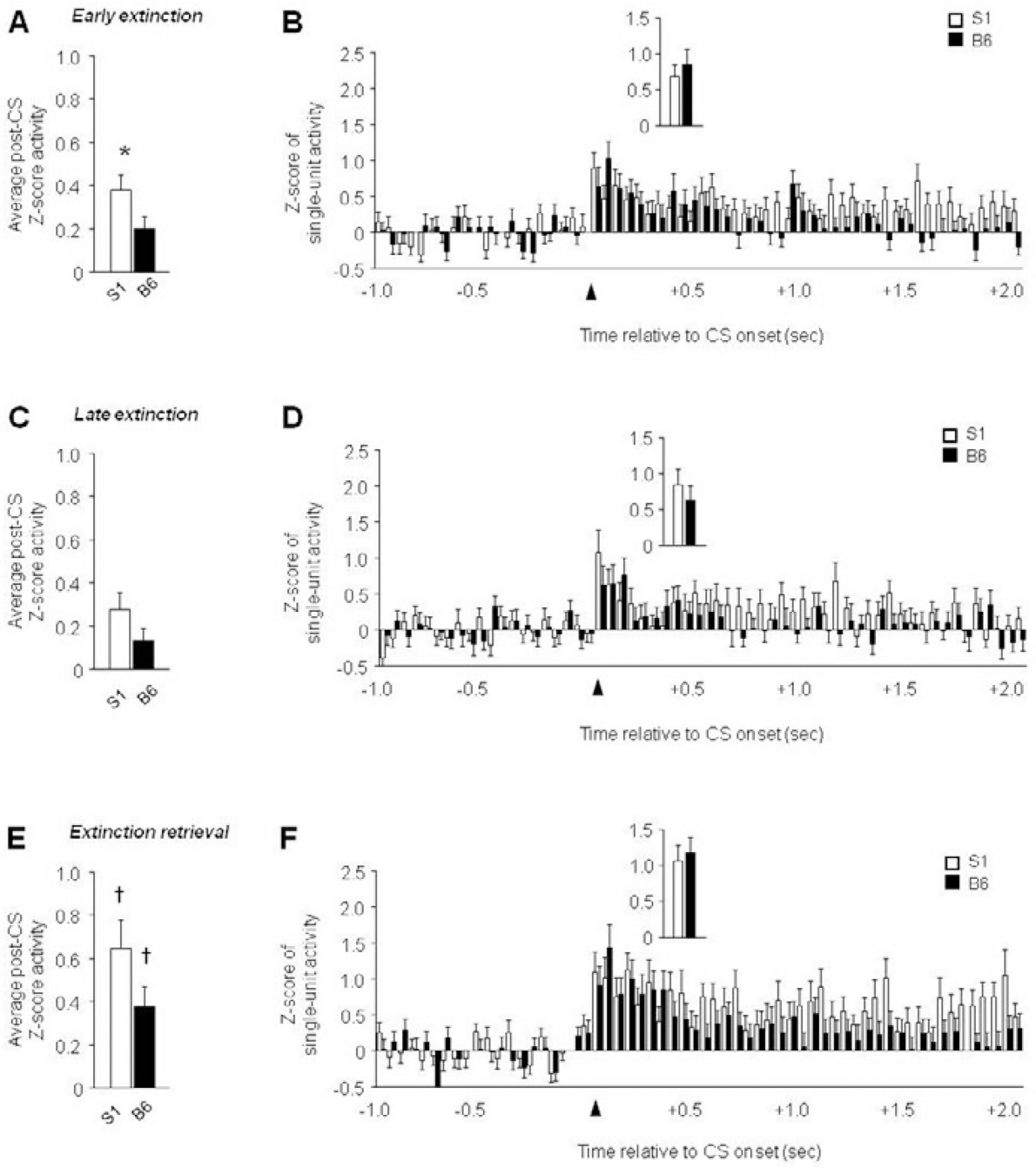

Figure 3. 'Paradoxically' high vmPFC single-unit activity in extinction-impaired S1 mice

(**A**) Higher average post-CS-related single-unit firing during early extinction in S1 mice, relative to B6 mice. (**B**) Peri-event histogram of CS-related single-unit firing during early extinction (first 100 msec, inset). (**C**) Average post-CS-related single-unit firing during late extinction. (**D**) Peri-event histogram of CS-related single-unit firing during late extinction (first 100 msec, inset). (**E**) Higher average post-CS-related single-unit firing during extinction retrieval than late extinction in S1 mice and B6 mice. (**F**) Peri-event histogram of CS-related single-unit firing during extinction retrieval (first 100 msec, inset). n=6–7 mice

per strain, n=43–52 units per test phase and strain. Data are Means ± SEM. * $P<.05$ versus B6/same taskphase, † $P<.05$ retrieval versus late extinction.

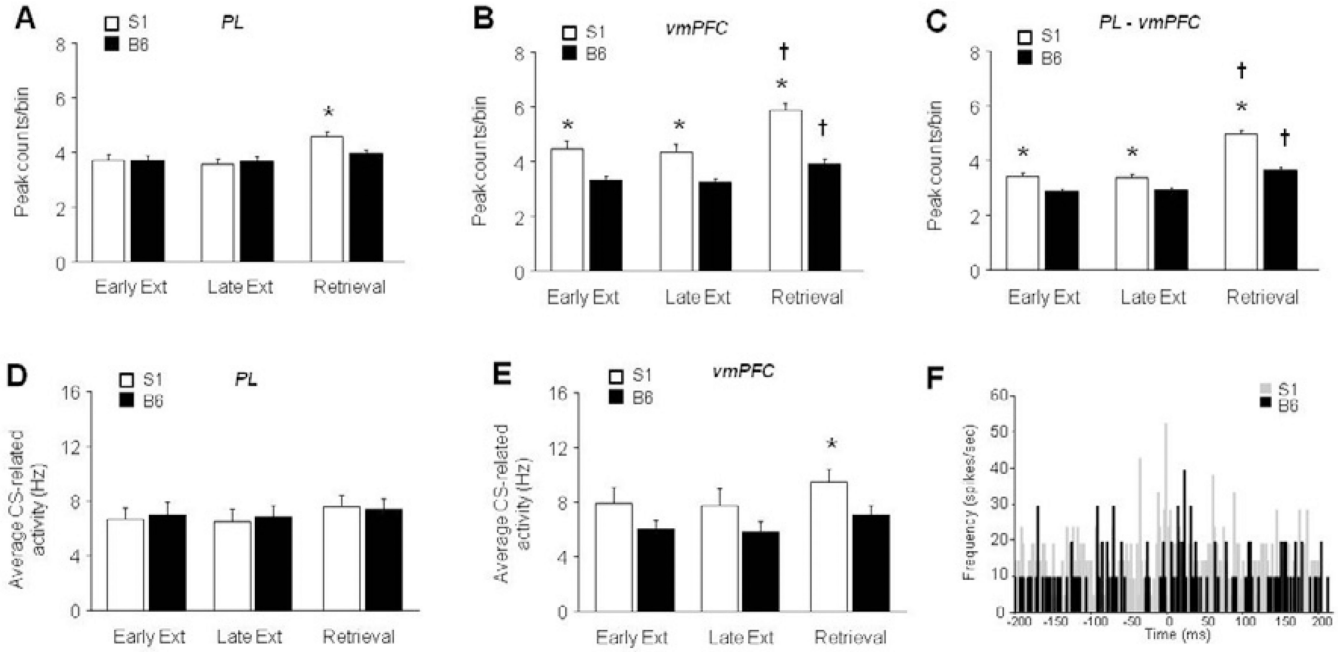

Figure 4. Increased correlated unit activity in the PL and vmPFC of S1 mice

(**A**) Cross-correlations were significantly higher in S1 than B6 mice during extinction retrieval, but not other phases. (**B**) Correlations were significantly higher in S1 than B6 mice during all test phases, and significantly higher in both S1 and B6 mice during retrieval than early extinction. (**C**) Correlations between the regions were significantly higher in S1 than B6 mice during all test phases, and significantly higher in both S1 and B6 mice during retrieval relative to early extinction. (**D**) Single-unit firing rate in the PL did not differ between strains at any testing phase. (**E**) Single-unit firing rate was significantly higher in S1 mice than B6 during extinction retrieval, but not early or late extinction training. (**F**) Example cross-correlograms from two vmPFC units in an S1 versus two in a B6 mouse. n=6–7 mice per strain, n=43–52 units per test phase and strain, n=285–2032 spike comparisons per strain per test phase. Data are Means ± SEM. * $P<.05$ versus B6/same task-phase, † $P<.05$ retrieval versus early extinction/same strain.

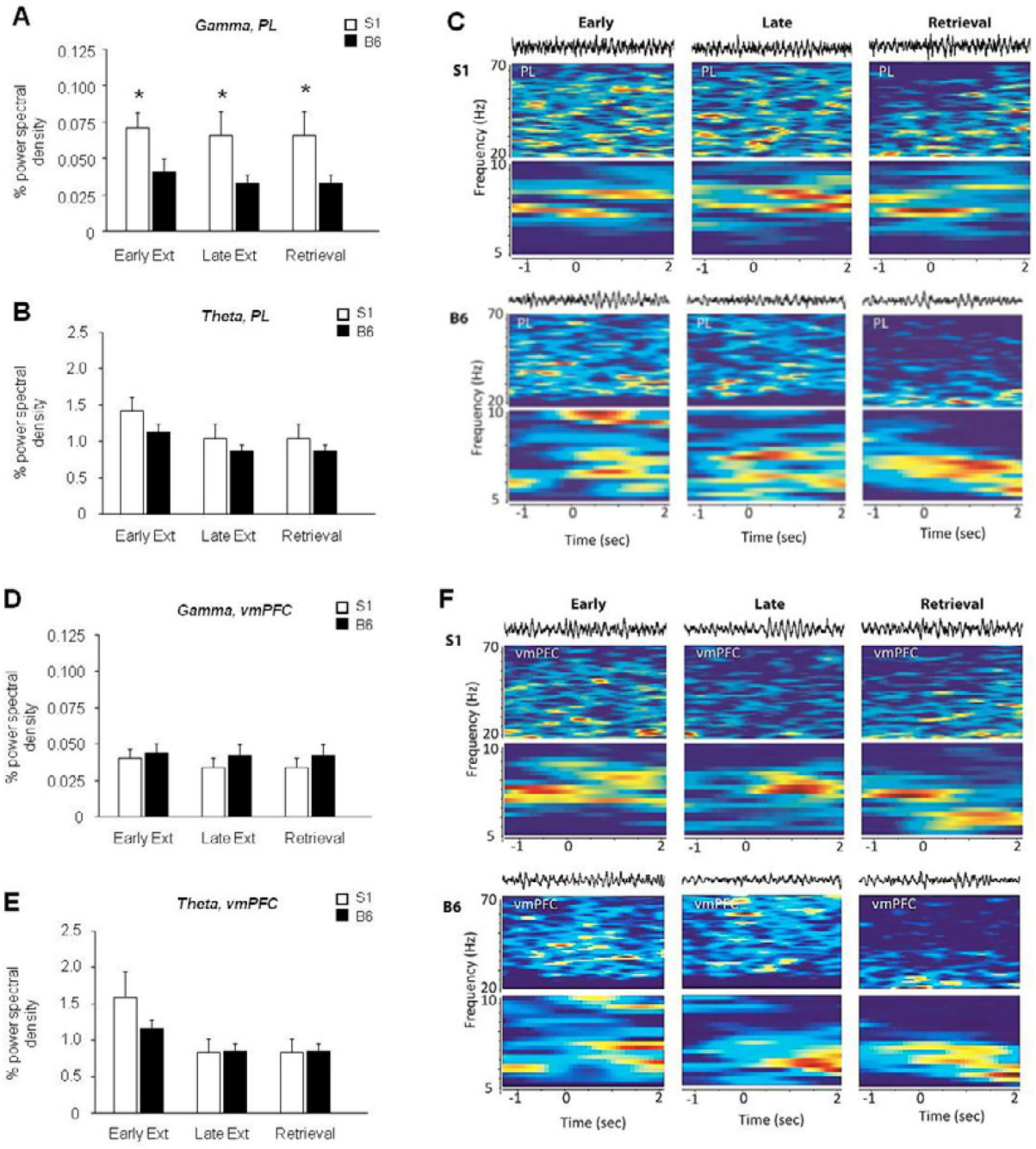

Figure 5. Increased gamma power in the PL of S1 mice

(**A**) S1 mice showed significantly higher gamma power than B6 mice in the PL during all phases of testing. (**B**) Theta power in the PL did not differ across strains or test phases. (**C**) Example waveforms and spectrograms from an S1 mouse and a B6 mouse. (**D**) Gamma power in the vmPFC did not differ across strains or test phases. (**E**) Theta power in the vmPFC did not differ across strains or test phases. (**f**) Example waveforms and spectrograms from an S1 mouse and a B6 mouse. n=6–7 mice per strain. Data are Means ± SEM. * *P*<.05 versus B6/same task-phase.

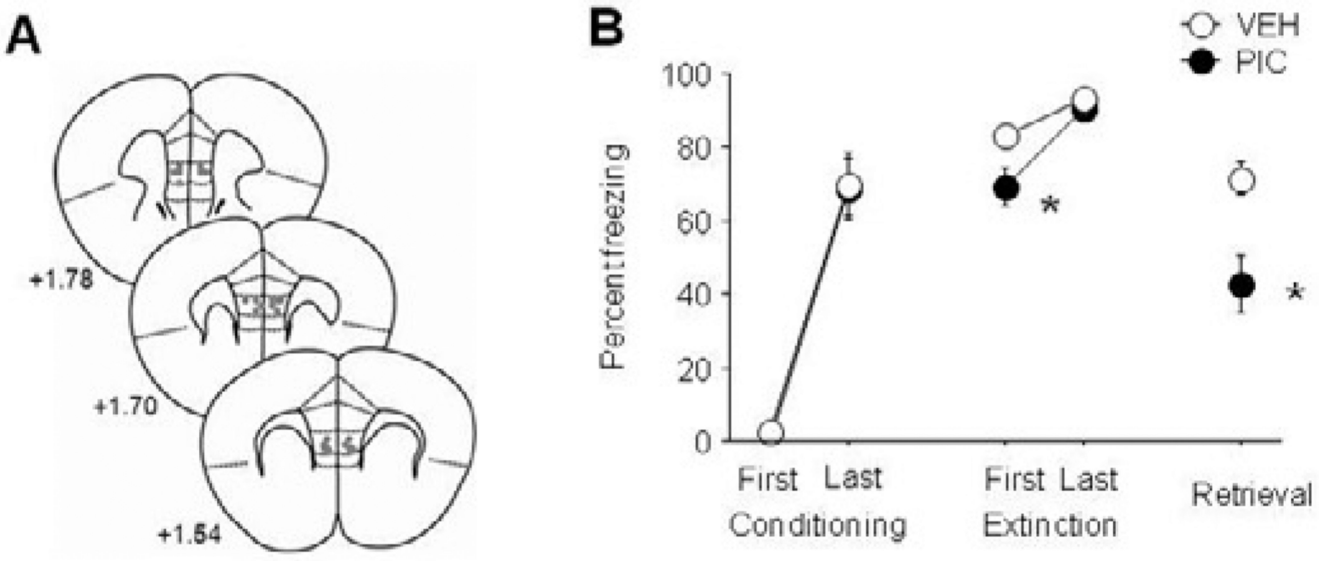

Figure 6. Pharmacological activation of the IL reduces fear and rescues extinction in S1 mice

(**A**) Infusion sites. (**B**) Lesser fear during early extinction and extinction retrieval in S1 mice infused with picrotoxin (PIC) than vehicle (VEH) controls. n=8–9 per group. Data are Means ± SEM. * $P<.05$ versus vehicle.

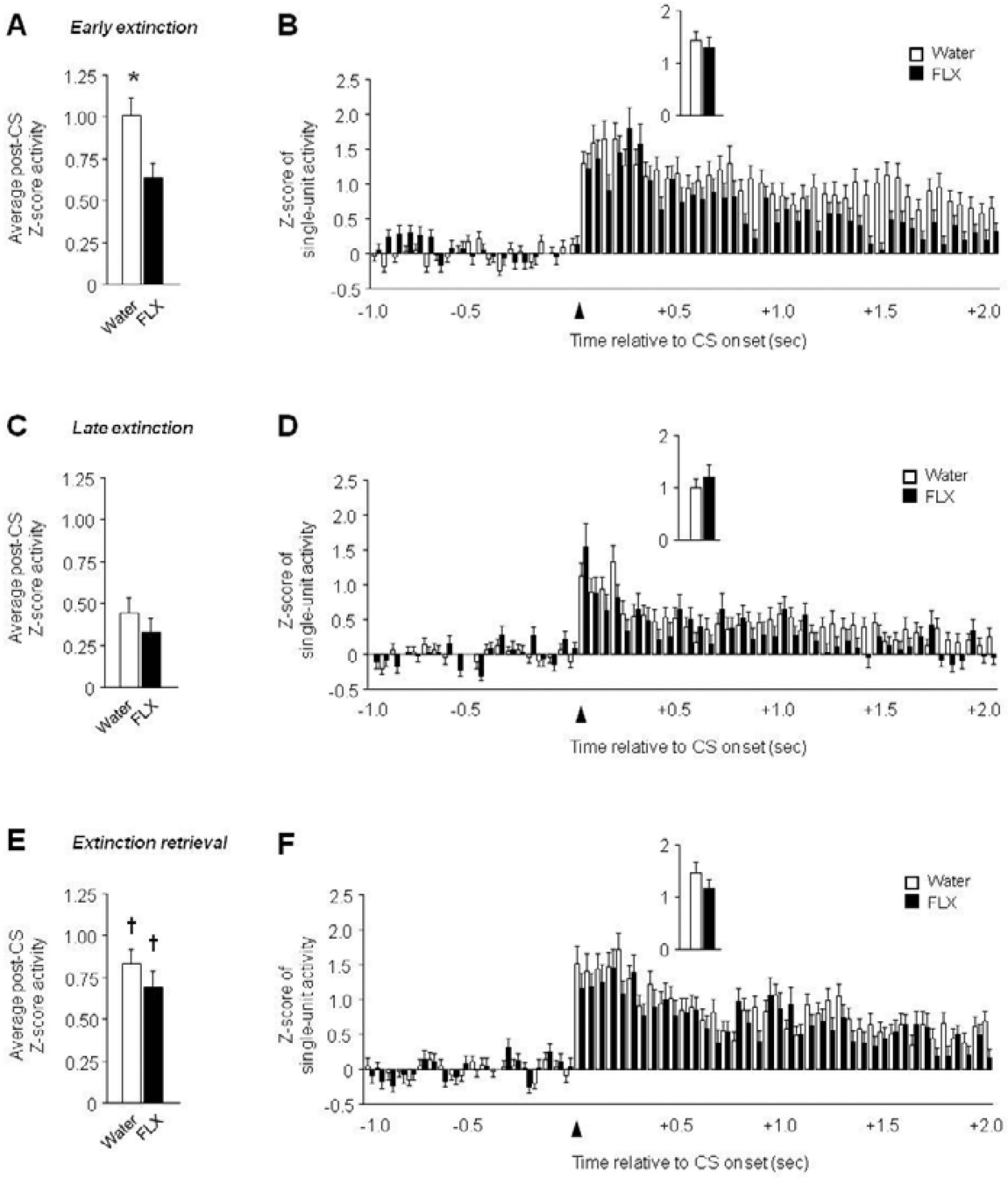

Figure 7. Limited effect of chronic fluoxetine treatment on abnormal vmPFC single-unit activity in S1 mice

(**A**) Lower average post-CS-related single-unit firing during early extinction in fluoxetine (FLX)-treated mice, relative to water controls. (**B**) Peri-event histogram of CS-related single-unit firing during early extinction (first 100 msec, inset). (**C**) Average post-CS-related single-unit firing during late extinction. (**D**) Peri-event histogram of CS-related single-unit firing during late extinction (first 100 msec, inset). (**E**) Higher average post-CS-related single-unit firing during extinction retrieval than late extinction in FLX-treated mice and

water controls. (**F**) Peri-event histogram of CS-related single-unit firing during extinction retrieval (first 100 msec, inset). n=5–8 mice per treatment, n=82–136 units per test phase and treatment. Data are Means ± SEM. * $P<.05$ versus fluoxetine/same task-phase, † $P<.05$ retrieval versus late extinction.

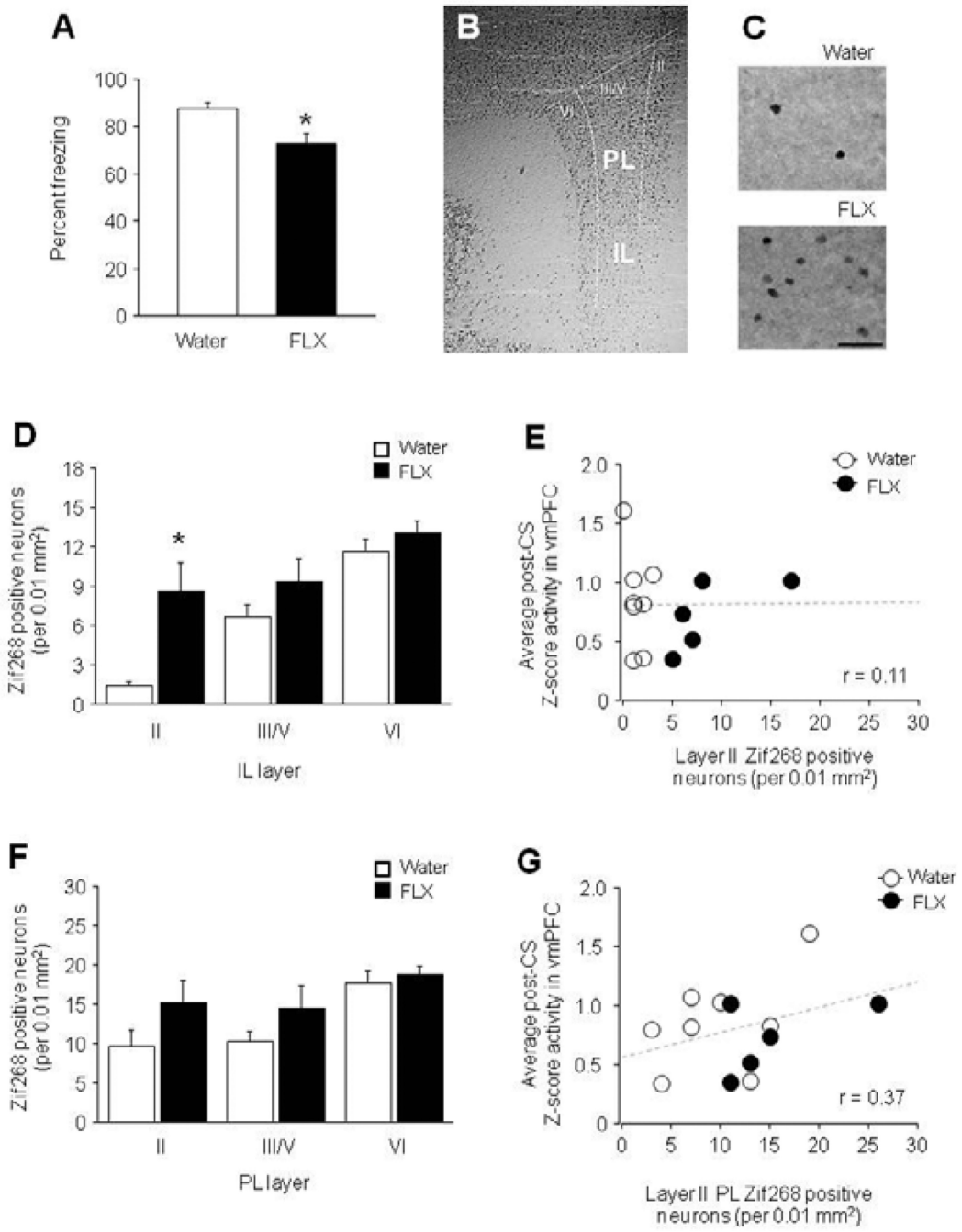

Figure 8. Increased immediate-early gene expression in fluoxetine-treated S1 mice

(**A**) Freezing during extinction retrieval was significantly lower in fluoxetine (FLX)-treated mice than water controls. (**B**) Zif268-labeled tissue showing anatomical demarcation of IL and PL and the layers within each region. (**C**) Examples of Zif268-labeled tissue in layer II of the IL in FLX-treated mice and water controls. (**D**) The number of Zif268-labeled cells after extinction retrieval was significantly higher in layer II of the IL in FLX-treated mice relative to water controls. (**E**) The number of Zif268-labeled cells in layer II of the IL did not significantly correlate with the post-CS firing of vmPFC single-units during extinction

retrieval. (**F**) The number of Zif268-labeled cells following extinction retrieval did not significantly differ between water and fluoxetine-treated mice in any layer of PL, although a trend was evident in layer II. (**G**) The number of Zif268-labeled cells in layer II of PL did not significantly correlate with the post-CS firing of vmPFC single-units during extinction retrieval. n=5–8 mice per treatment. Data are Means ± SEM. * $P<.05$ versus water in the same task-phase or layer. Data are Means ± SEM.